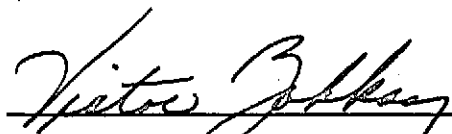NEW YORK UNIVERSITY

Center for Interdisciplinary Programs

Grant NGR-33-016-179

SEMI ANNUAL REPORT

1 March 1973 through 31 August 1973

VICTOR ZAKKAY

Assistant Director, Aerospace Laboratory

REYNOLDS NUMBER AND MACH NUMBER EFFECT ON SPACE SHUTTLE CONFIGURATIONS

Analytical studies have been conducted concerning the lee-surface flow phenomena over a space shuttle orbiter model based on the experimental data obtained during September, 1971 through August, 1972 , (Ref. 1). Lee-surface peak heating phenomena and flow separation patterns were analyzed. The major results of analyses are briefly presented.

1. LEE-SURFACE HEAT TRANSFER DISTRIBUTIONS

It is very difficult to estimate lee-surface heat transfer distributions theoretically over three-dimensional body configurations such as the space shuttle orbiter at large angles of attack, since little is known about flow properties in a separated flow region.

In order to check the order of magnitude of lee-surface heat transfer rates, some estimates have been made based on the measured surface pressure distribution and two-dimensional or axisymmetric boundary layer assumptions, neglecting cross flow effects. Two extreme entropy relations were used to determine the local flow conditions; the local inviscid stagnation pressure was assumed constant at the value behind the normal shock and the conical shock.

The results of heat transfer calculations are presented in Fig. 1 for a typical test condition at $\alpha = 0^{\circ}$. As shown in this Figure, the difference in heat transfer based on both entropy relations is negligible for a laminar flow, while appreciably large for a turbulent flow. The modified Lees method (by Eckert and Tewfik, Ref. 2) was chosen for laminar calculations since this analysis eliminates the need for the assumption $\rho u = $ const. across the boundary layer by use of the reference enthalpy concept, thereby improving the accuracy of estimates. This method agrees quite well with the original

Lees method (Ref. 3) near the nose region. Turbulent heat transfer rates were calculated by using the Reshotko-Tucker method (Ref. 4) for both two-dimensional and axisymmetric flows along with the Flat Plate Reference Enthalpy Method (FPREM) by Eckert (Ref. 5) for a two-dimensional flow.

It is observed in the Figure (Fig. 1) that there is no significant difference in heat transfer estimates between axisymmetric and two-dimensional flows for a turbulent boundary layer. Moreover, FPREM (Ref. 5) applied locally agrees very well with the Reshotko-Tucker method with conical shock (Ref. 4) which takes into account the effect of pressure gradient. Zakkay and Callahan (Ref. 6) have shown that heat transfer rates for a turbulent boundary layer in a mild adverse pressure gradient can be predicted with reasonable accuracy by FPREM. Hoydysh and Zakkay (Ref. 7) also showed that turbulent heat transfer rates in a strong pressure gradient are predicted fairly well by this method.

In view of these previous observations and present calculated results, the Reshotko-Tucker method (two-dimensional case) with conical shock entropy and FPREM with both entropy relations were used to estimate the turbulent heat transfer rates for $\alpha > 0^{\circ}$. This estimate was based on the measured pressure distribution of the nearest Reynolds number corresponding to each heat transfer test, assuming an attached boundary layer flow on the lee-surface of the orbiter model.

The lee-surface heat transfer results are plotted for different values of angle of attack with the Reynolds number as a parameter in Figs. 2 through 6, to determine the effect of Reynolds number on heat transfer rates at each angle of attack. In these Figures the maximum and minimum values of analytical estimates corresponding to the test Reynolds numbers are shown. Only two-dimensional estimates are included here for turbulent heat transfer calculations because of the reason explained above. Also, separation points determined from oil flow studies are shown in these Figures.

2

At $\alpha = 0^o$, as shown in Fig. 2, laminar boundary layer flow is believed to exist over the major part of the lee-surface. Although the space shuttle orbiter is a three-dimensional body and the laminar estimates (Ref. 2) assumes a highly cooled wall with the negligible effect of local pressure gradient, the laminar axisymmetric calculation agrees well with experiments in front of the shoulder section. Behind the shoulder, flow appears to be more two-dimensional type than axisymmetric, and the boundary layer changes from laminar to transitional, with a resulting scattering in measurements.

At $\alpha = 10^o$ Fig. 3, the boundary layer before the shoulder starts to change from laminar to turbulent as the Reynolds number increases. At the highest Reynolds number, the boundary layer is believed to have become turbulent, and the magnitude of the maximum heat transfer rate is about the same order of magnitude as the values predicted by two-dimensional turbulent analyses. This tendency becomes more pronounced at $\alpha = 20^o$ Fig. 4, where the boundary layer is changed from laminar to transitional at low Reynolds numbers and to turbulent at high Reynolds numbers. For both $\alpha = 10^o$ and 20° , separation occurs after the expansion over the shoulder. This suggests that the peak heating at small angles of attack ($\alpha = 10^o$, 20°), is due to the boundary layer transition, but not due to flow separation for the Reynolds number range tested here. At $\alpha = 20^o$, another heating peak appears behind the separation point, typical in a separated flow region.

For high angles of attack ($\alpha = 30^o$, 40° , peak heating phenomena associated with flow separation, termed the vortex-induced peak heating, are observed (Figs. 5, 6). In both cases, the maximum heating values are found to be nearly the same order of magnitude as the local turbulent heat transfer rates calculated from boundary layer analyses with measured surface pressure distributions. Therefore, lee-surface flow near the location of peak heating is believed to be similar to reattached flow. It is confirmed from oil flow studies that the feather-like

3

reattachment surface pattern does correspond to a high (peak) heating region. At large angles of attack ($\alpha = 30^{\circ}, 40^{\circ}$), it is also observed that after the strong expansion over the shoulder heat transfer rates again reach nearly the same order of magnitude as local turbulent heating values.

2. PEAK HEATING PHENOMENA

Maximum and secondary peak heat transfer rates obtained for varying Reynolds numbers and angles of attack are analyzed in Figs. 7 through 9. In Fig. 7 the peak heating is plotted as a function of Reynolds number $R_{\infty,L}$ where a distinction is made between the peak heating within a separated flow region and that due to boundary layer transition as determined with the aid of oil flow studies. The same data are plotted against the local Reynolds number $R_{\infty,x}$ in Fig. 8. Both Figures show that peak heating values due to transition are strong functions of Reynolds number and increase with both $R_{\infty,L}$ and rapidly over the Reynolds number range covered here, while peak heatings within a separated flow region do not correlate; the values even tend to decrease slowly with Reynolds numbers ($R_{\infty,L}$, $R_{\infty,x}$). This result contradicts somewhat the previous investigation (Langley data, Ref.8) where the peak heating (vortex induced peak heating) increases with Reynolds numbers ($R_{\infty,L}, R_{\infty,x}$). However, the present result for peak heating due to the boundary layer transition shows a similar trend to that of Langley data (Ref. 8), while the peak heating within a separated flow region does not show such a similar correlation in terms of Reynolds number.

A recent experimental investigation (Ref. 9) on a similar orbiter model with a canopy showed lower lee-surface heat transfer values than those of Ref. 8 and also a lack of correlations in terms of Reynolds number and angle of attack. The level of lee-surface heat transfer of Ref. 9 is even lower than the present test results (see Ref. 1 for the experimental results with a canopy), but the overall trends of both results are similar. The reason for the inconsistent results and

4

large scattering for peak heating values obtained for each of these experiments is not known at present.

The location of peak heating plotted against $R_{\infty,L}$ (Fig. 9) indicates almost no dependence on $R_{\infty,L}$ in good agreement with the Langley data (Ref. 8). For some Reynolds numbers at $\quad$ in the present test, there is no sharp heating peak, instead a heating plateau appears as shown in Fig. 9.

Detailed analyses of the lee-surface heat transfer and surface pressure data indicate that the pressure field does not contribute to the peak heating phenomenon; the peak heating is not caused by an abrupt increase in surface pressure, as already observed in the previous investigation(Ref. 8).

At relatively low angles of attack ($\alpha = 10^{\circ}$, 20°), the laminar boundary layer exists over the lee-surface of the nose section before the shoulder at low Reynolds numbers. As the Reynolds number increases, the transition point moves forward, resulting in higher heating value (peak heating) attained before the flow undergoes an abrupt expansion over the shoulder section. Since there is no significant Reynolds number effect on the pressure field (i.e. there is no viscous interactions) before the shoulder, flow starts to expand at almost the same position for all Reynolds numbers where the boundary layer is still transitional or has just become turbulent. Therefore, a simple correlation of the peak heating due to the boundary layer transition and the Reynolds number is obtained, while its location is insensitive to the Reynolds number. As mentioned above, the overall trend of so-called vortex-induced peak heating of the Langley data(Ref. 8) is similar to this type of (transitional) peak heating in the present study, although the absolute values of heat transfer are different.

The peak heating due to vortex-surface interactions, vortex-induced peak heating, is observed at high angles of attack ($\alpha = 20^{\circ}$, 30°, 40°) This type of peak heating is caused by the thinning of the viscous shear layer as a result of

5

outflow induced by the vortices, as characterized by a feather-like reattachment surface pattern in oil flow pictures.

As shown in Figs. 43 and 44, the vortex-induced peak heating in the present investigation was found to be insensitive to Reynolds numbers $(R_{\infty,L}, R_{\infty,x})$, in contrast to the previous result of Ref. 8. Although the full explanation of the discrepancies between the two sets of data are not yet known, one possible reason may be the different methods of heat transfer measurements. The thin wall technique was used in the present investigation, while the phase-change-paint technique was employed in Ref. 8. Also, it can be understood that the body geometry and surface roughness are important factors in determining the peak heating, if it is classified into two types; the peak heating due to the boundary layer transition and the vortex-induced peak heating. To interpret the experimental results from different sources correctly and apply them to the space shuttle design, it is necessary to resolve this data acquisition problem. It is noted here, based on the comparisons of various data, that lower heat transfer rates are obtained by the thin wall technique over those by the paint technique.

3. OIL FLOW STUDIES AND SEPARATION PATTERNS

It was found from oil flow studies that the separation at relatively low angles of attack $(\alpha = 10^{\circ}, 20^{\circ})$ is of a "free vortex layer" type in terms of Maskell's separation models in three-dimensional flow. On the other hand, the separation type on the front part is considered to be a "bubble" type at high angles of attack $(\alpha = 30^{\circ}, 40^{\circ})$.

The nose part of the space shuttle mode at $\alpha = 30^{\circ}$ is magnified and presented in Fig. 10 to show an example of the bubble type separation which starts at a singular point. In this Figure the feather-like high shear (heating) region near the leeward centerline is clearly observed following the separated flow region immediately behind the singular point. This high shear region, a kind of

6

reattachment flow region, is created by a vortex-surface interaction and it is here that the vortex-induced peak heating phenomenon is observed in heat transfer measurements. It is also seen that this high shear region is followed by another separated flow region corresponding to a low heat transfer region as confirmed by heat transfer data.

The bubble type separation has not yet been obtained experimentally although it was anticipated theoretically. However, it should be noted here that this type of separation is followed by a free vortex layer type separation. This fact will partly explain why it is difficult to obtain a bubble type separation pattern on a blunt-nosed flight vehicle.

Additional oil flow studies have been conducted over sharp and blunt cones. The general trend of the results were found to be similar to that on a space shuttle configuration. The bubble type separation was also observed on the nose part of a blunt cone as shown in Fig. 11.

Based on the present oil flow studies, Maskell's separation models and Wang's extended analysis(Ref. 10)were found to be compatible with present experimental results.

4. INVISCID FLOW ANALYSIS OVER HIGHLY YAWED CONES

The numerical analysis developed by Kutler et al.(Ref. 11)was modified slightly and applied successfully to calculate inviscid flowfield over highly yawed coned involving internal shocks. It was found from several sample calculations that there is a viscous displacement effect for a highly yawed cone in hypersonic flows. This effect is relatively small before the primary separation, which means attached flow with thin boundary layer. In the separated flow region of the leeward surface, however, the displacement effect becomes significant due to vortex interactions. Therefore, the inviscid flow analysis cannot be applied to this region directly unless some corrections for this viscous effect on the pressure field are made.

7

To account for this effect the "near surface", defined as the fictitious surface which gives the same pressure distribution as in experiments, was found by this inviscid flow analysis. A sample calculation shown here corresponds to one of the McElderry's experiments (Ref. 12); $M_\infty = 6$, $\theta_c = 6^\circ$, $\alpha = 9^\circ$. After several trial and error calculations a circular-elliptical cone connected at $\varphi = 125^\circ$ was found to give practically the desired pressure distribution, where the major axis of the ellipse if 1.14 compared to the radius of circle of 1.0. The calculated pressure distribution is presented in Fig. 12 along with the numerical solution for a circular cone and experimental data. The change in pressure due to this small modification of the surface contour is seen to be significant; the surface pressure distribution calculated over the modified cone is in good agreement with the experimentally obtained pressure distribution on the original circular cone.

From the above sample calculation, it is found that the effect of vortex interactions on the pressure field in a separated flow region over a highly yawed cone can be evaluated by an inviscid flow analysis if an appropriate fictitious surface ("near" surface) is found corresponding to the actual surface pressure distribution on the circular cone. The surface flow calculated by an inviscid flow analysis over this fictitious cone describes fairly well the actual surface flow phenomena on the original circular cone. Therefore, it is concluded that a good inviscid flow analysis, corrected for the viscous displacement effect, offers a powerful means to calculate the "essentially conical" flow involving separation.

REFERENCES

1. Zakkay, V., Miyazawa, M., and De Simone, G., "Reynolds Number and Mach Number Effect on Space Shuttle Configuration," Final Report of NASA Grant, New York University, Sept. 1972.

2. Eckert, E.R.G. and Tewfik, O.E., "Use of Reference Enthalpy in Specifying the Laminar Heat-Transfer Distribution Around Blunt Bodies in Dissociated Air," Journal of the Aero/Space Sciences, Vol. 27, No.6, June 1960, pp.464-466.

3. Lees, L., "Laminar Heat Transfer over Blunt-Nosed Bodies at Hypersonic Flight Speeds," Jet Propulsion, Vol. 26, No.4, April 1956, pp. 259-269.

4. Reshotko, E. and Tucker, M., "Approximate Calculation of the Compressible Turbulent Boundary Layer with Heat Transfer and Arbitrary Pressure Gradient," NACA TX-4154, 1957.

5. Eckert, E.R.G., "Engineering Relations for Friction and Heat Transfer to Surfaces in High Velocity Flow," Journal of the Aeronautical Sciences, Vol. 22, No.8, Aug. 1955, pp. 585-587.

6. Zakkay, V. and Callahan, C.J., "Laminar, Transitional, and Turbulent Heat Transfer to a Cone-Cylinder-Flare Body at Mach 8.0," Journal of the Aerospace Sciences, Vol. 29, NO. 12, Dec. 1962, pp.1403-1420.

7. Hoydysh, W.G. and Zakkay, V., "An Experimental Investigation of Hypersonic Turbulent Boundary Layers in Adverse Pressure Gradient," AIAA Journal, Vol. 7, No.1, Jan. 1969, pp. 105-116.

8. Hefner, J.N., "Lee-Surface Heating and Flow Phenomena on Space Shuttle Orbiters at Large Angles of Attack and Hypersonic Speeds," NASA TN D-7088, 1972.

9. Bertin, J.J. et al., "The Effect of Nose Geometry on the Aerothermodynamic Environment of Shuttle Entry Configurations," Texas University at Austin, Aerospace Engineering Report No. 73001, 1973.

10. Wang, K. C., "Separation Patterns of Boundary Layer over an Inclined Body of Revolution," AIAA Paper No.71-130, 1971. (Also, AIAA Journal, Vol. 10, No. 8, Aug. 1972, pp. 1044-1055.)

11. Kutler, P., Reinhardt, W.A., and Warming, R.F., "Numerical Computation of Multishocked, Three-Dimensional Supersonic Flow Fields with Real Gas Effects," AIAA Paper No. 72-702, 1972.

12. McElderry, E.D., Unpublished Data, 1972, Aerospace Research Labs., Wright-Patterson Air Force Base, Ohio.

Fig. 1

HEAT-TRANSFER HEAT-TRANSFER CALCULATIONS
BASED ON MEASURED PRESSURE DISTRIBUTION
$M_\infty = 6$, $\alpha = 0°$

$R_{\infty,L} \approx 0.7 \times 10^7$

$T_{0\infty} \approx 850 °R$

AXISYMMETRIC   TURBULENT

2-DIMENSIONAL

AXISYMMETRIC

2-DIMENSIONAL

LAMINAR

AXISYMMETRIC

2-DIMENSIONAL
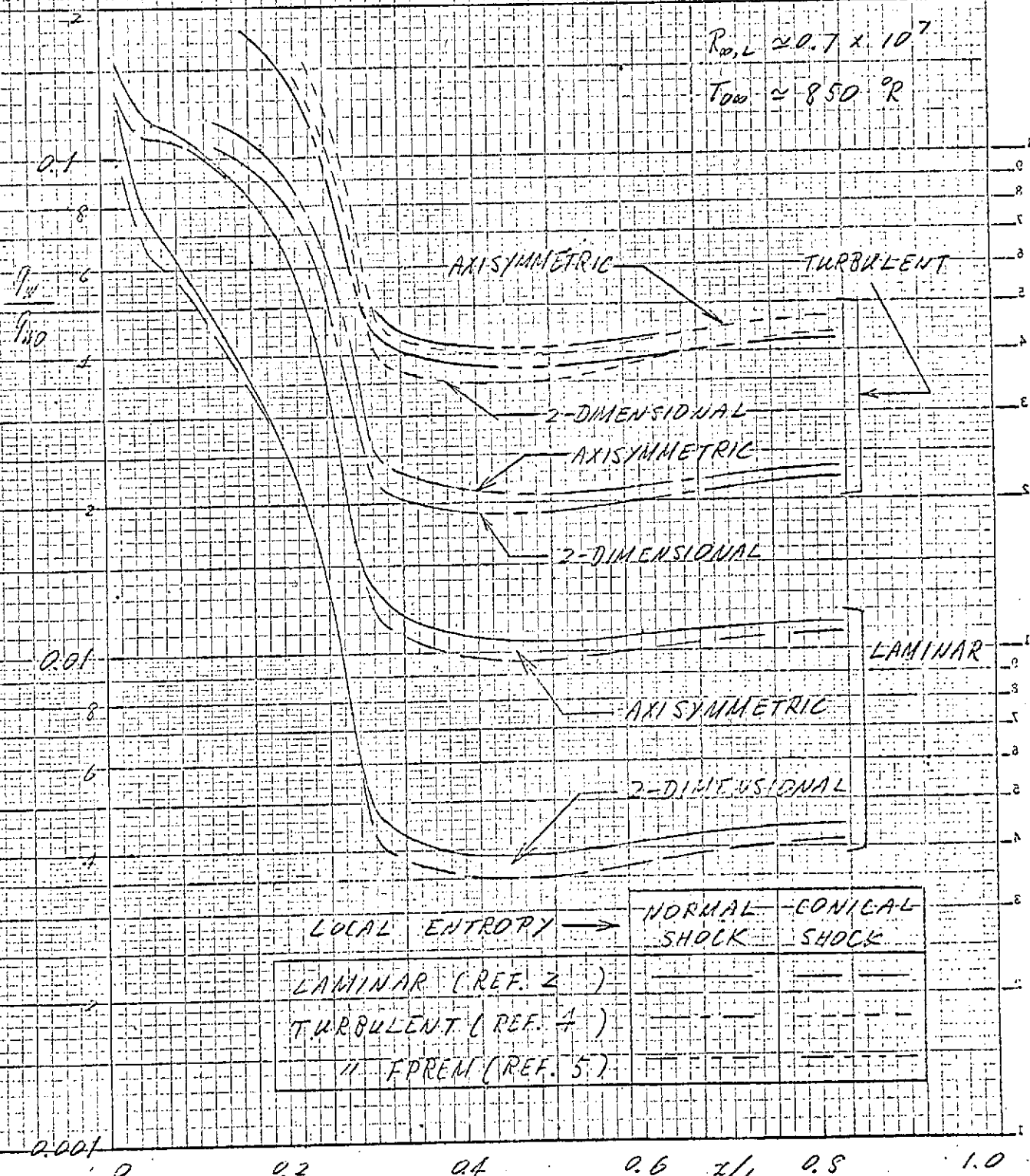
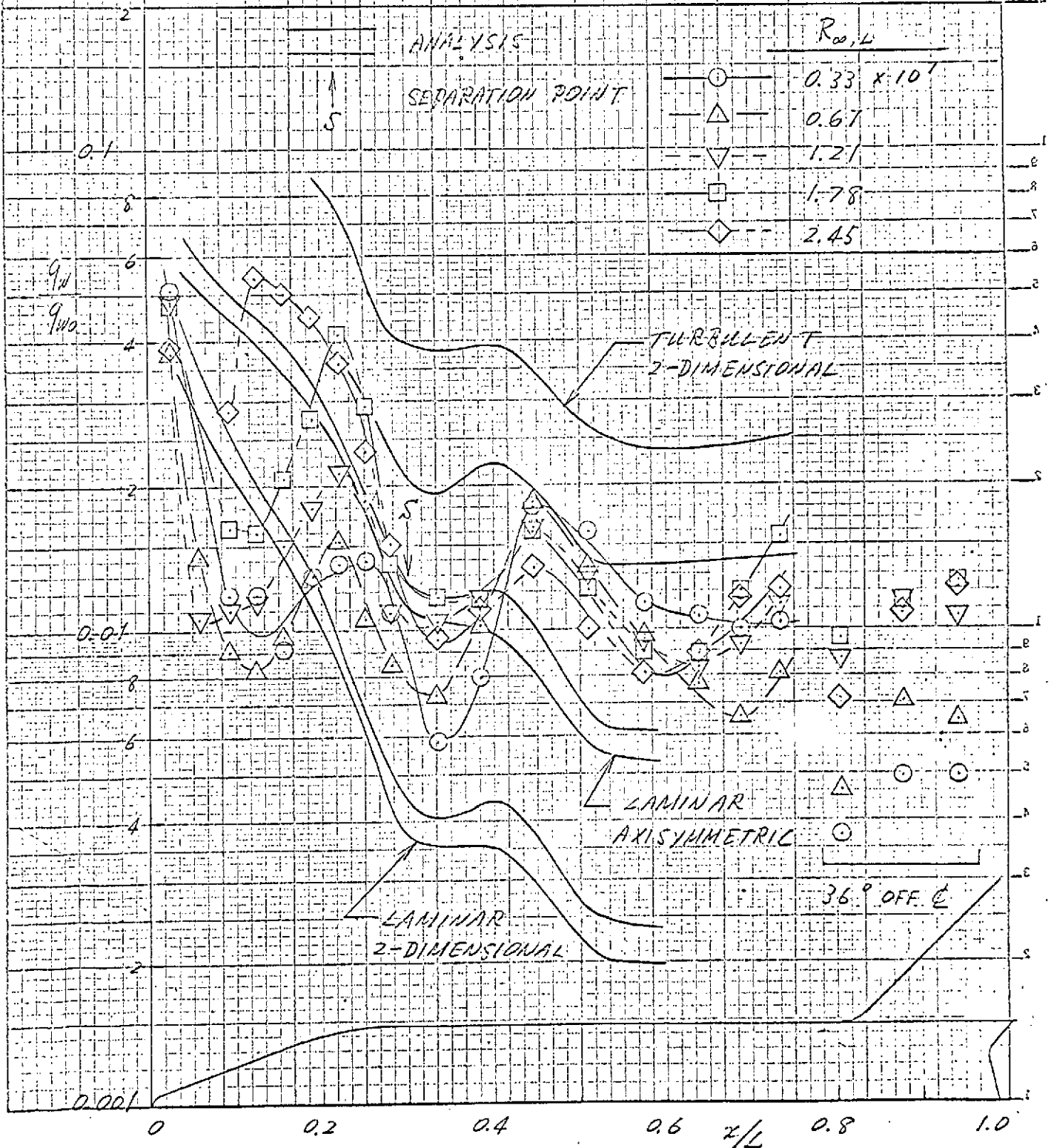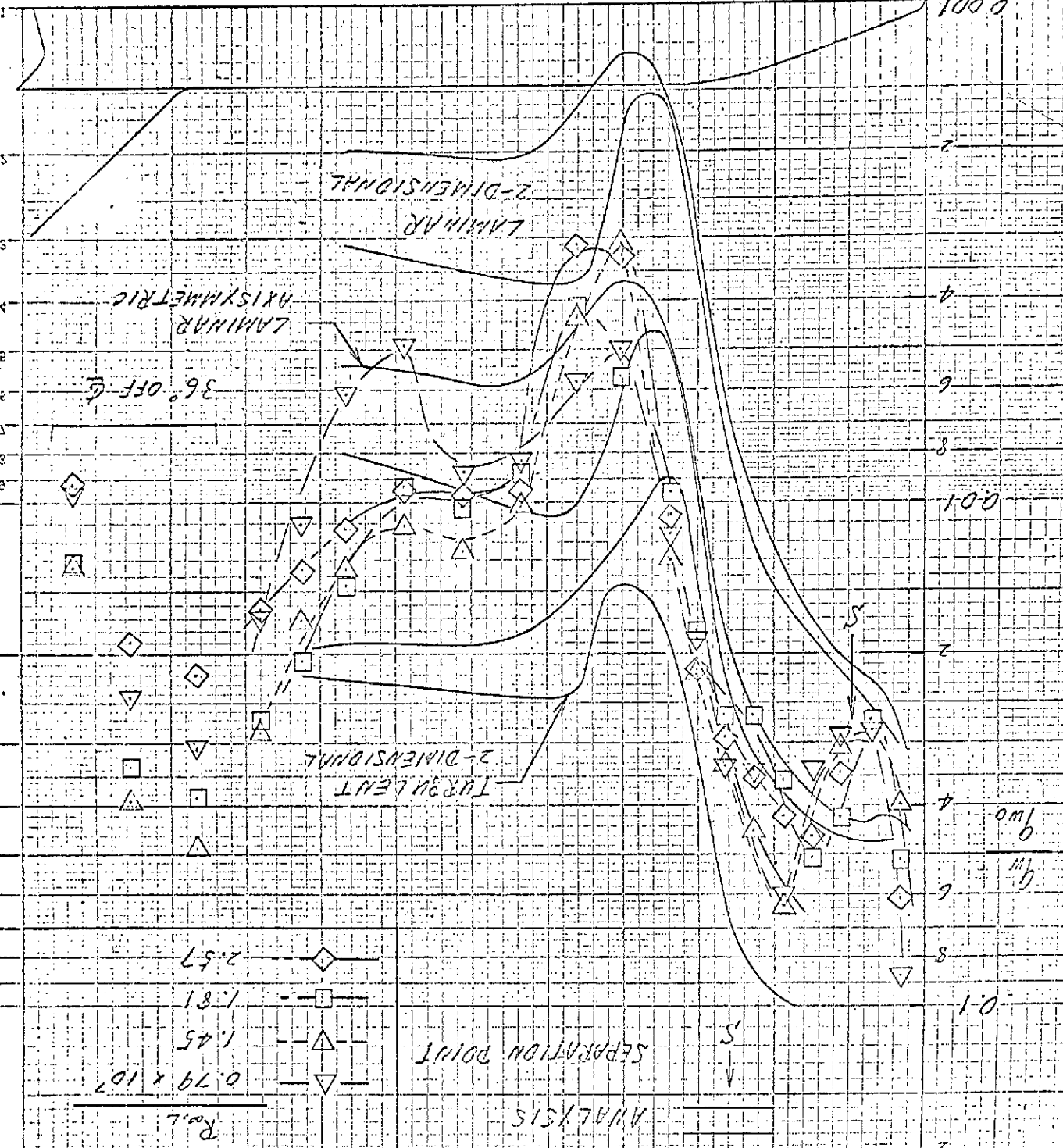| LOCAL ENTROPY →	NORMAL SHOCK	CONICAL SHOCK
LAMINAR (REF. 2)		
TURBULENT (REF. 4)		
" FPREM (REF. 5)		

Fig-2
HEAT TRANSFER ALONG THE LEEWARD CENTERLINE
$M_\infty = 6$, $\alpha = 0^\circ$

Fig. 3

HEAT TRANSFER ALONG THE LEEWARD CENTERLINE

$M_\infty = 6, \quad \alpha = 10°$
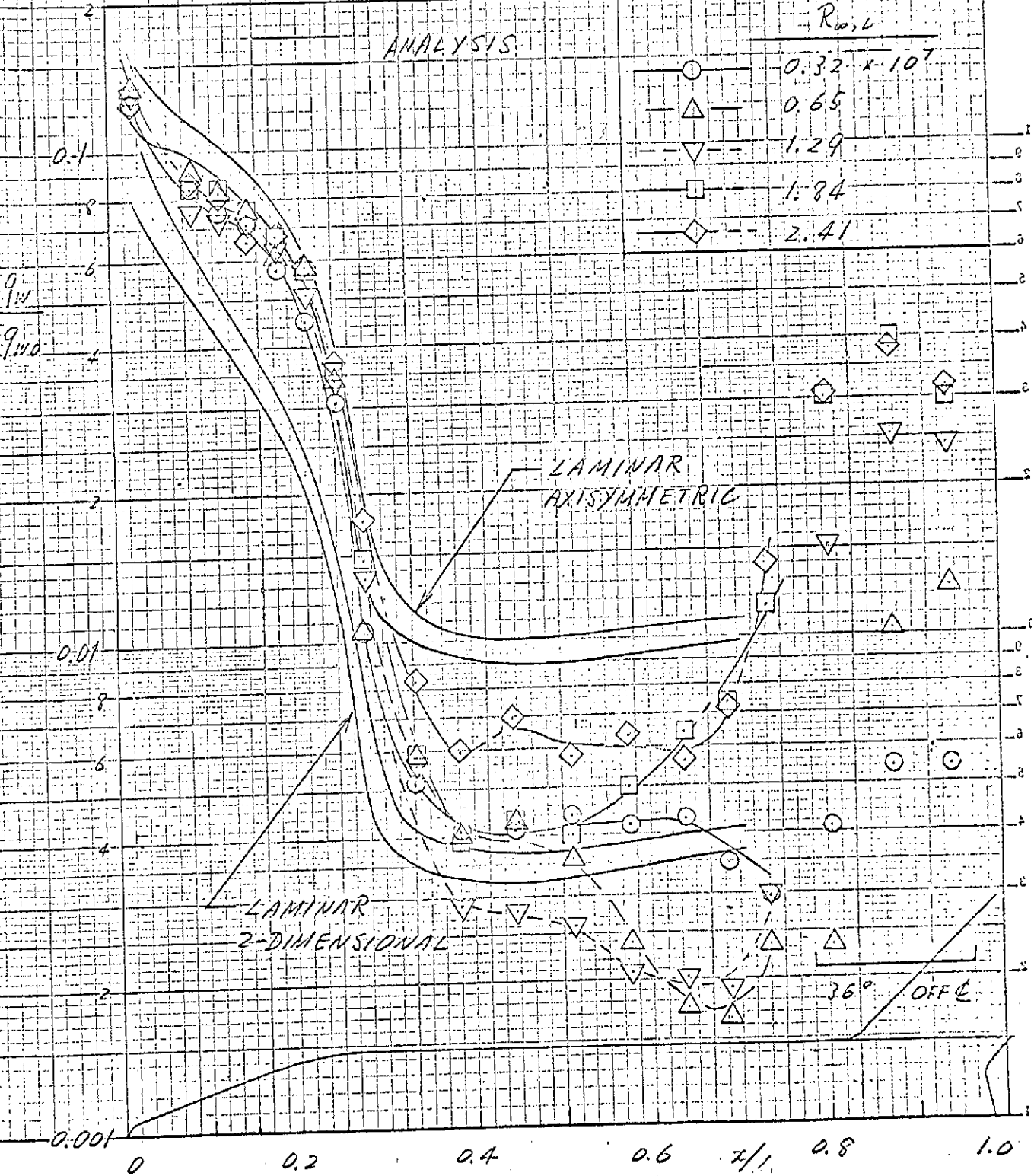
Fig. 4

HEAT TRANSFER ALONG THE LEEWARD CENTERLINE

$M_\infty = 6$, $\alpha = 20°$

ANALYSIS
SEPARATION POINT

	$R_{\infty,L}$
⊙	0.33×10^7
△	0.67
▽	1.21
□	1.78
◇	2.45

TURBULENT 2-DIMENSIONAL

LAMINAR AXISYMMETRIC

3.6° OFF $\mathcal{C}$

LAMINAR 2-DIMENSIONAL

$\dfrac{q_w}{q_{wo}}$

x/L

HEAT TRANSFER ALONG THE LEEWARD CENTERLINE

Fig. 5

$M_\infty = 6,\ \theta = 30°$

SEPARATION POINT

ANALYSIS

	$Re_{\infty,L}$
	0.79×10^7
	1.45
	1.81
	2.57

LAMINAR AXISYMMETRIC

LAMINAR 2-DIMENSIONAL

TURBULENT 2-DIMENSIONAL

36° OFF-ℂ

x/L

Fig. 6

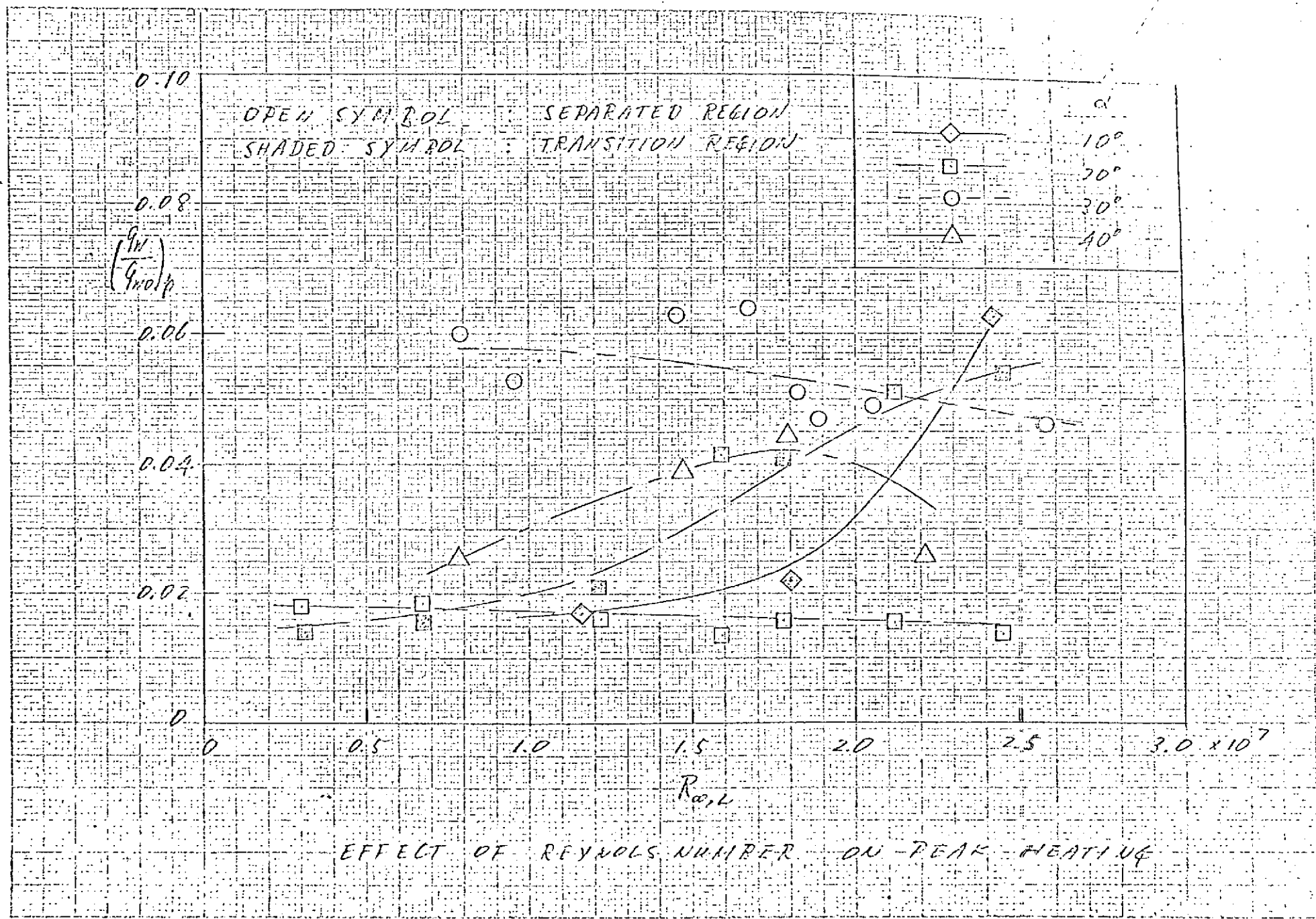HEAT TRANSFER ALONG THE LEEWARD CENTERLINE

$M_\infty = 6, \quad \alpha = 40°$
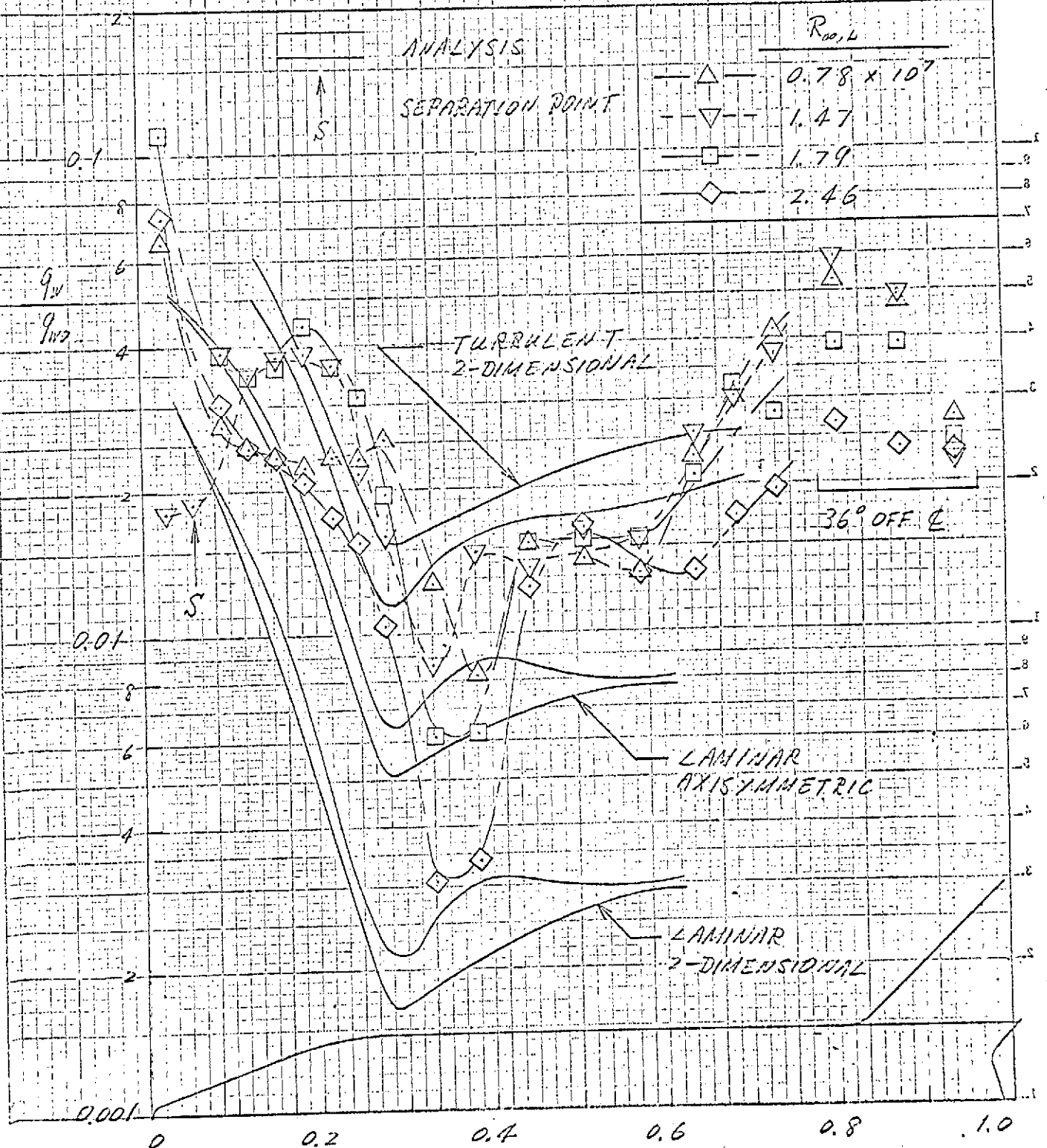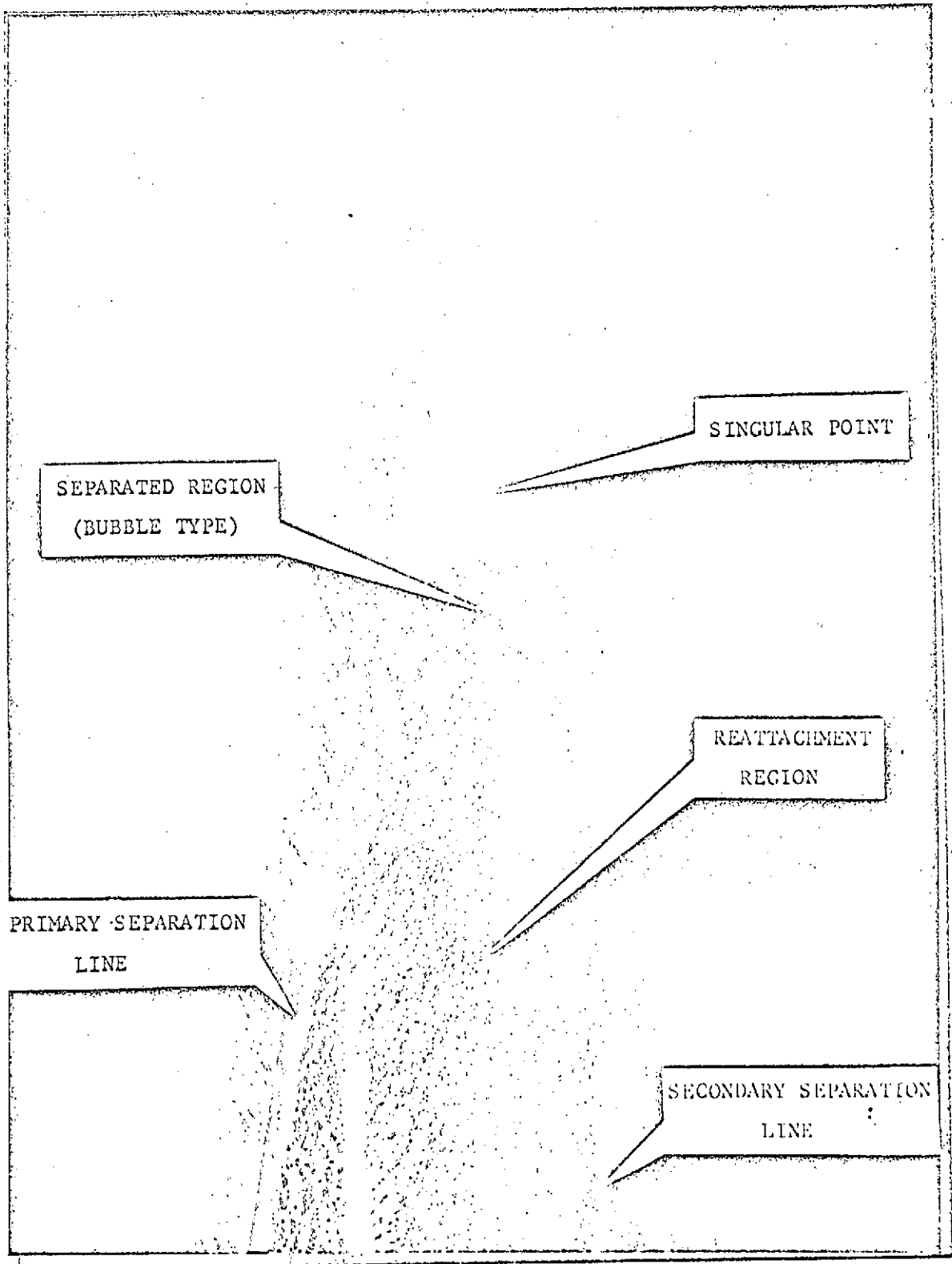
Fig. 7
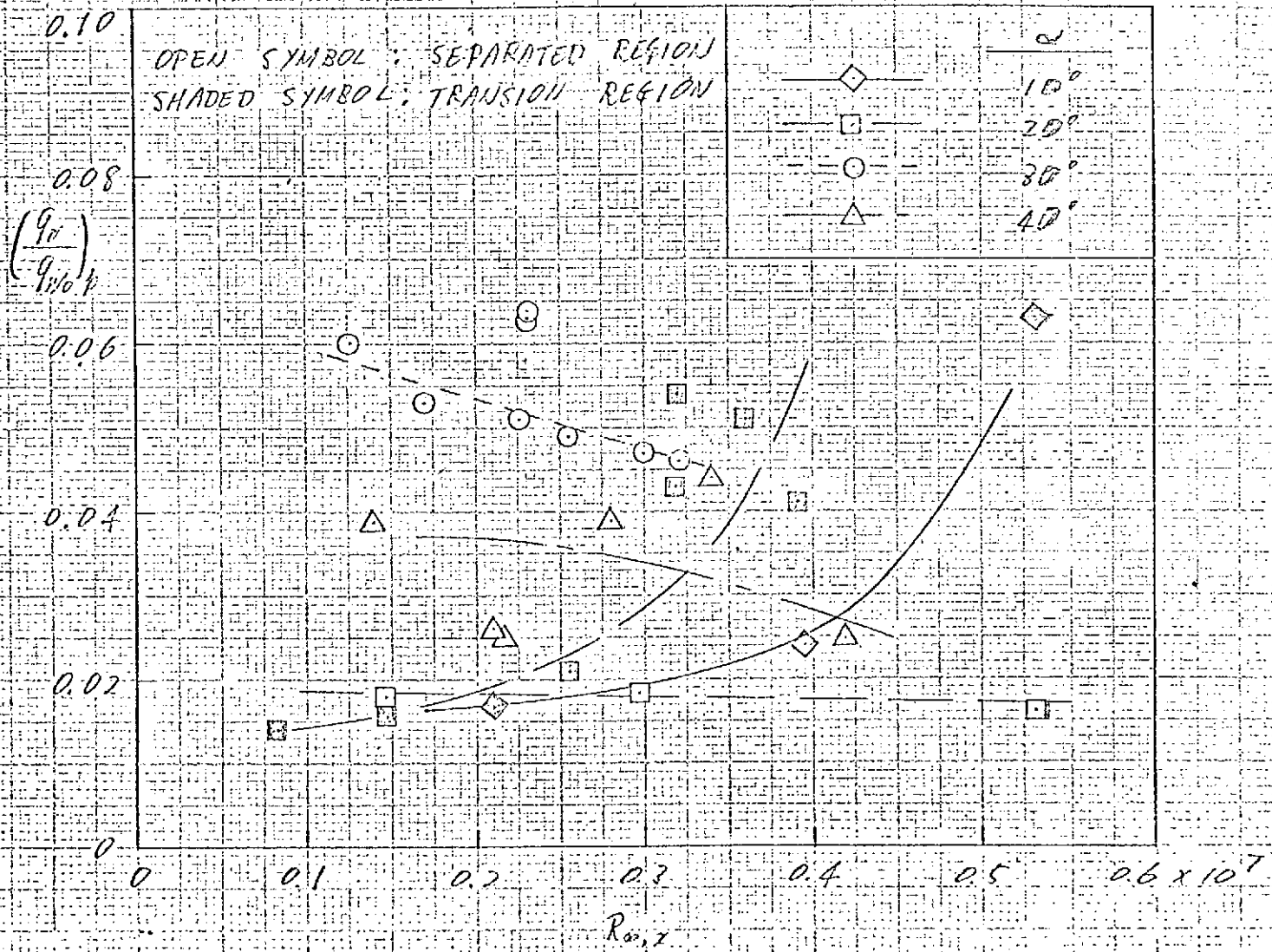
EFFECT OF LOCAL REYNOLDS NUMBER ON PEAK HEATING

Fig. 8

Fig. 9

SINGULAR POINT

SEPARATED REGION
(BUBBLE TYPE)

HIGH HEATING
REGION

PRIMARY SEPARATION
LINE

SECONDARY SEPARATION
LINE

$\alpha = 30^{\circ}, \quad R_{\infty,L} = 1.43 \times 10^{7}$

Fig. 10

SINGULAR POINT

SEPARATED REGION
(BUBBLE TYPE)

REATTACHMENT
REGION

PRIMARY SEPARATION
LINE

SECONDARY SEPARATION
LINE
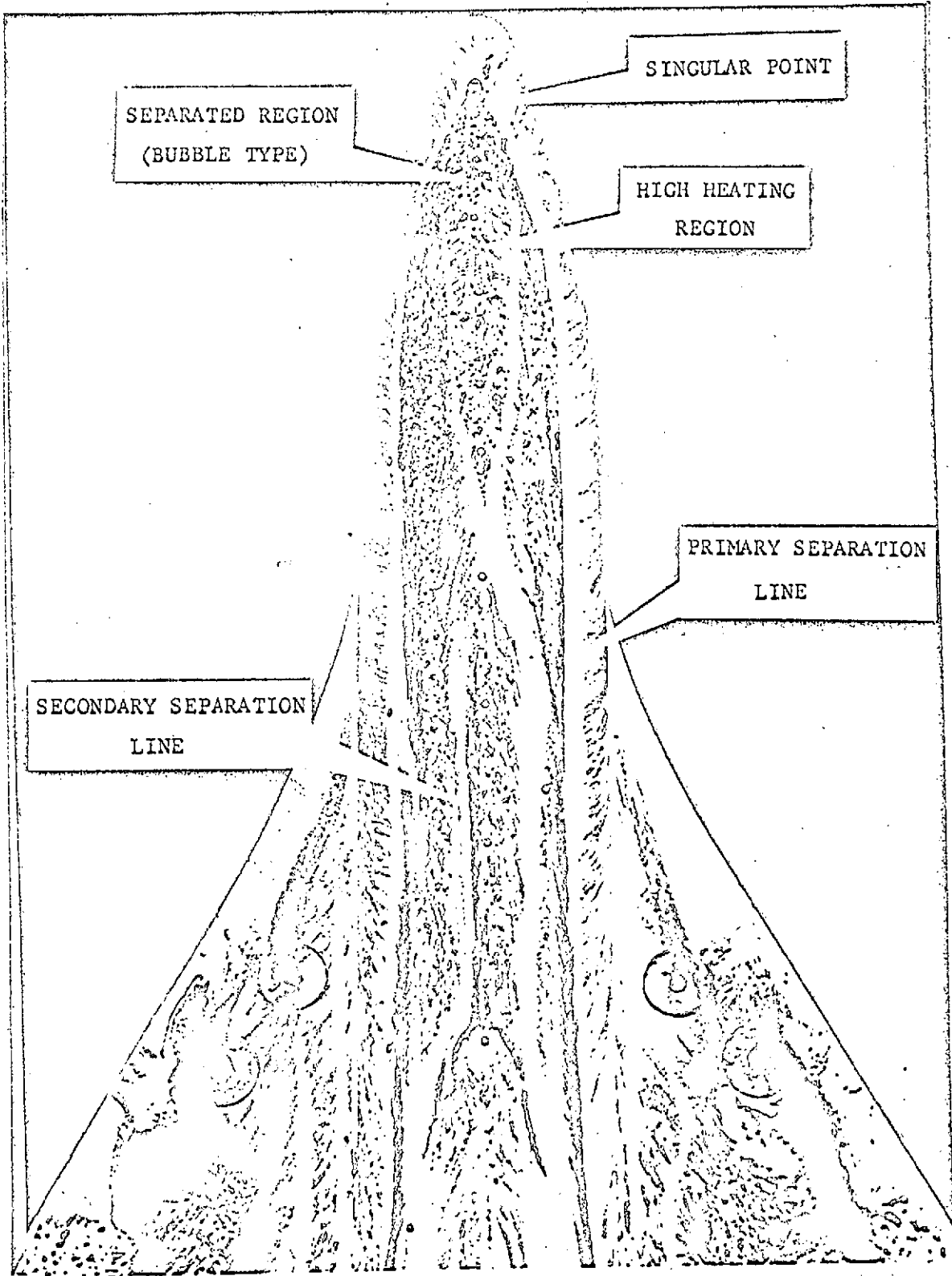
$\alpha = 20^{\circ}, \quad \alpha/\theta_c = 2.67, \quad R_N/R_B = 0.24, \quad R_{\infty} = 3.53 \times 10^7 \quad 1/ft$

Fig. 11

Fig. 12